



RESEARCH ARTICLE

Graphene oxide modifications induced by excimer laser irradiations

Alfio Torrisi^{1,2}  | Luciano Velardi¹ | Antonio Serra^{1,2} | Daniela Manno^{1,2} |
Lorenzo Torrisi^{2,3}  | Lucio Calcagnile^{1,2}

¹Department of Mathematics and Physics “E. De Giorgi”—CEDAD (Center of applied physics, Dating and Diagnostics), University of Salento, Lecce, Italy

²Sections of Lecce and Catania, INFN, Lecce, Italy

³Department of Mathematical and Computer Sciences, Physical Sciences and Earth Sciences, MIFT, University of Messina, Messina, Italy

Correspondence

Alfio Torrisi, Department of Mathematics and Physics “E. De Giorgi”—CEDAD (Center of applied physics, Dating and Diagnostics), University of Salento, 73 100 Lecce, Italy.
Email: alfio.torrisi@unisalento.it

Funding information

Universita del Salento

The properties of graphene oxide foils were modified by excimer laser irradiation at different fluences and times. The irradiations were performed in air and in vacuum using a pulsed UV laser operating at 248-nm wavelength and 23-ns pulse duration. Measurements of ablation yield, microscope surface morphology and Raman spectroscopy were performed. The residual surface shows a significant oxygen reduction due to the removing of functional oxygen groups, a thickness reduction due to the removal of graphene layers depending on the used laser shots and a presence of defects in the graphene sheets as evident by the Raman spectroscopy investigation.

KEYWORDS

excimer laser, graphene oxide, laser ablation, Raman spectroscopy, reduced graphene oxide

1 | INTRODUCTION

Graphene is an atomically thin, two-dimensional (2D) sheet of sp^2 carbon atoms in a [honeycomb structure](#). It has been shown to have many interesting properties such as high biocompatibility,¹ high mechanical strength and flexibility,² high electrical and thermal [conductivity](#),³ molecular barrier abilities,⁴ special optical properties,⁵ and other remarkable physical and chemical properties. For these reasons, it has been the goal of countless research efforts to realize different devices based on graphene (sensors, dosimeters, prostheses, etc.) and to incorporate graphene into polymers to design polymer-based nanocomposites.^{6–8} The deposition of relatively large graphene monolayers with low defects concentrations is possible by using different methods, for example, Chemical Vapor Deposition (CVD) and Physical Vapor Deposition (PVD) techniques with sophisticated controls in high vacuum conditions.⁹

A simple and inexpensive method to prepare graphene oxide (GO) foils, rich in water and functional groups of oxygen, which can be

converted into graphene-like foils containing micrometric sheets in graphene, consists in the deposition of graphene oxide water dispersion at different concentrations. The solidification of the colloidal solution permits to prepare micrometric and sub-micrometric graphene oxide films. The physical and chemical properties of GO are very different of the graphene, but processes of reduction using thermal annealing, laser irradiation, and ionizing radiation allow to produce reduced GO (rGO) films and foils with properties similar to those of graphene, depending on their level of reduction.^{10,11}

GO is an insulator material, with high absorbance and low reflectivity in the visible region, rich in water and carbonyl, epoxydic, hydroxylic, and carboxylic groups. Usually, GO is used as a raw material for mass production of graphene via reduction. However, under different conditions, the types and arrangements of oxygen-containing groups in GO can be varied, giving excellent and controllable physical properties, such as tunable electronic and mechanical properties depending on the oxidation degree, enhanced electrical and thermal conductivity, optical transparency and fluorescence, and

This is an open access article under the terms of the [Creative Commons Attribution-NonCommercial-NoDerivs](#) License, which permits use and distribution in any medium, provided the original work is properly cited, the use is non-commercial and no modifications or adaptations are made.

© 2022 The Authors. *Surface and Interface Analysis* published by John Wiley & Sons Ltd.

nonlinear optical properties. Based on these outstanding properties, many electronic, optical, optoelectronic, and thermoelectric devices with high performance can be achieved based on GO and different reduction levels of rGO.^{12,13}

The peculiar properties make graphene, GO, and rGO attractive candidates for different applications going from biomedicine to engineering, from nuclear physics to microelectronics and from environment to cultural heritage fields.^{14–19}

The presence of defects may affect the performance of such devices. Radiations, temperature, and chemical etching may induce damage in graphene foils. Soft and hard X-rays, energetic ions and electron beams, neutrons, laser beams and thermal annealing can easily break the sp^2 bond structure forming defects in graphene that is weakly bound to the substrate. Multilayer graphene, grown on silicon carbide (SiC) and other substrates, after ionizing irradiation in air or in vacuum generate defects on their bulk and surface depending on the absorbed dose.²⁰

GO has a similar hexagonal carbon structure to graphene but the different functional groups of oxygen are responsible for many advantages over graphene, including higher solubility, electrical insulation and the possibility to realize a functional surface for use in nanocomposite materials. Graphene derivatives have proven to be effective fillers in polymer nanocomposite materials thanks to their ideal material properties and dispersibility in polymer matrices, which has led to many applications. The tight packing of sp^2 carbon atoms has been shown to serve as a near-perfect barrier to gas molecules, which demonstrates its use in packaging materials, protection for sensitive electronic devices, corrosion-resistant materials and realization of nanofilters and membranes.²¹ The fine tuning of the filler content in nanocomposites, in fact, can be used to adjust the selectivity of certain-sized molecules to generate superior membrane technologies.²²

GO laser irradiation is drastically modified by the laser irradiation and its changes depend on the laser parameters^{23–25} (pulse energy and duration, wavelength, and fluence) and irradiation conditions (vacuum, air, gas, and focalization). For instance, significant difference occurs if the irradiation is performed in air or in vacuum, generally producing high oxygen reduction effects in vacuum and oxidation effects in air, as reported in the literature.^{26–28} In this work, we focus on the study on defect generation in graphene, induced by exposure to an ultraviolet (UV) excimer laser, emitting 23-ns pulses at 248-nm wavelength. We compare the irradiation of GO substrates in air and under vacuum, showing through Raman spectroscopy, that, defects are introduced in both cases, at different rates. The experimental results are important to show the damage-creating mechanisms upon photon interaction as well as designing graphene-based components for UV lithography systems.

2 | MATERIALS AND METHODS

GO thin foils were obtained using the colloidal solution in water at 0.4% GO concentration furnished by Graphenea.²⁹ Thin sub-micrometric films were obtained depositing the solution on a rotating polymer substrate using the spin coating system; micrometric films

with a thickness around 10 microns were obtained by solution drop deposition and successive drying in air at 40°C. Deposited films and foils were detached from the polymer substrate using the lukewarm water float technique. The thin films were collected on aluminum frames while the 10 microns thick foils were self-supporting. Figure 1 shows examples of thin films (0.1 microns in thickness) (a), the 10 microns prepared GO foils (b) and the surface roughness acquired with a surface profiler of the GO foil (c).

The pristine GO has a density of 1.45 g/cm³, high thickness uniformity, and a surface roughness of the order of 1 micron or less. The GO irradiation was performed by an KrF pulsed laser (248-nm wavelength with 23-ns pulse duration, maximum pulse energy of 600 mJ) operating in single pulse or in repetition rate up to 10-Hz frequency. The laser intensity generally ranges between 10⁸ and 10¹⁰ W/cm², obtained using a laser spot focused diameter of about 200 μ m.

Literature reports that the absorption coefficient of 248 nm wavelength into graphite is about $\alpha = 16 \mu\text{m}^{-1}$.³⁰ Assuming this datum comparable with that into GO, the penetration depth of the laser penetration in the irradiated surface layers is of about $\delta = 1/\alpha = 0.063 \mu\text{m} = 63 \text{ nm}$.

The GO irradiation was realized in air (at 23°C, 1 atm and 50% humidity) and in high vacuum (10⁻⁵ mbar) with two different experiments, which similar set-ups which are reported in the schemes of Figure 2a and b, respectively. In both cases, laser pulse uses an energy from about 2 mJ up to about 400 mJ and a circular spot focalization with a large diameter of about 3 mm. The spot was maintained large to have irradiated areas suitable for successive physical analyses.

The UV laser irradiation produces a layer removing higher than the laser penetration depth because of the dense plasma produced at the solid-gas interface, very fast plasma expansion in air and in vacuum during the laser pulse interaction of 23-ns duration. The total removed thickness produced by single laser pulses was measured in terms of ablation yield given in μg GO matter per laser shot.

The GO film thickness was measured before and after the laser ablation using single or multiple laser shots. In order to study the surface modification induced by the UV laser irradiation, optical and electron microscopy was used to analyze the irradiated GO surfaces in detail. The surface roughness was measured with a surface profiler (Tencor P10) having a depth resolution of 1 nm.

Micron-Raman spectra were acquired with a Leica microscope using a Spectra Physics Ar⁺ ion laser operating at 514.5 nm, with a maximum power of 25 mW. The laser power on samples was about 0.125 mW. The analysis was performed on graphene oxide foils using a 2- μ m laser spot size focused on the sample surface by a 50 \times objective (Leica N-Plan 566027). Raman spectra were collected and analyzed with Renishaw Wire© software, supplied with the spectrometer. This software performs baseline correction and then removes the fluorescence background with a calculation method based on cubic spline interpolation.³¹ The typical vibrational modes of the carbon-based materials are evident in all the μ Raman spectra acquired on different ion beam irradiated GO samples between 900 and 2000 cm⁻¹ (D and G peaks) and between 2400 and 3400 cm⁻¹ (2D, D + G and C features). The first and second order Raman regions

FIGURE 1 Graphene oxide (GO) thin films with 0.1 microns thickness (A), GO thick foil with 10 microns thickness (B), and surface roughness measurement of a 10 micron GO film (C)

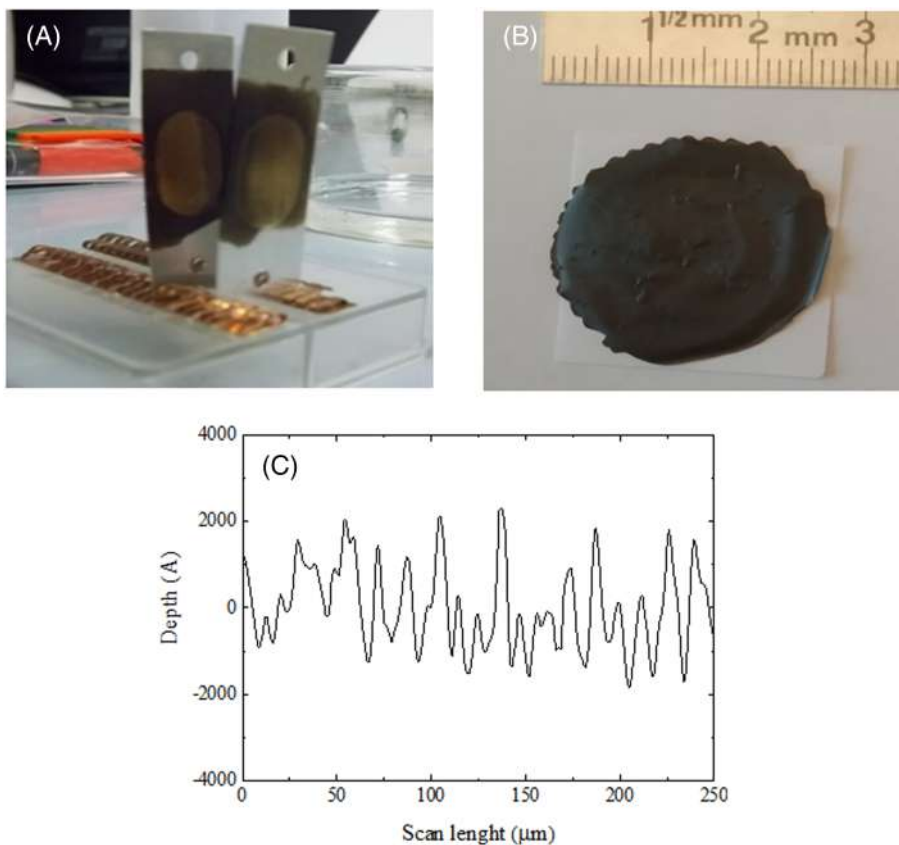
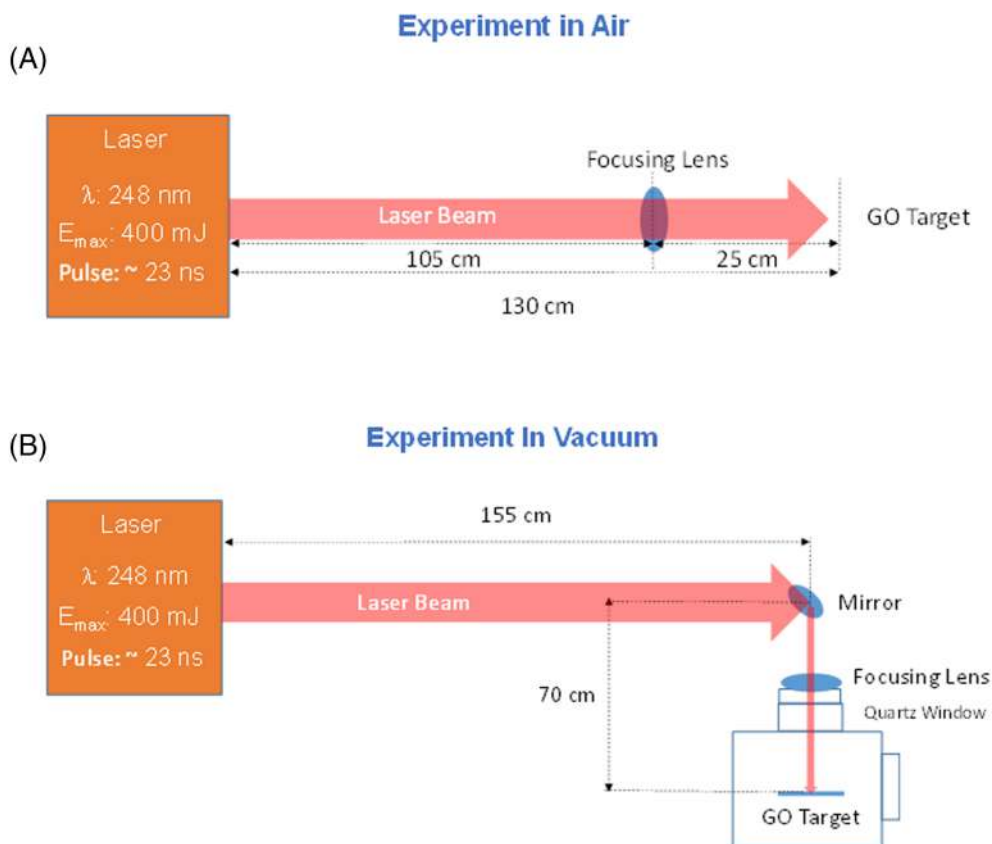


FIGURE 2 Experimental set up of graphene oxide (GO) irradiation in air (A) and in vacuum (B)



were fitted to Lorentzian curves, while PseudoVoigt function was used for the G band, by Fityk software.³²

3 | RESULTS

The microscope investigations of the prepared GO surface and of the UV laser irradiated surface are reported for comparison in the SEM images, at the same magnification, of Figure 3A for the pristine, Figure 3B for the sample irradiated in vacuum and in Figure 3C for that irradiated in air.

The first (Figure 3A) indicates that the surface is uniform and compact with a low roughness (less than 1 microns), the second (Figure 3B), obtained using in vacuum a single laser shot irradiation of 400-mJ pulse energy, shows small irregularities due to the laser erosion effects, the third, performed using the same energy of laser irradiation and single shot in air, shows remarkable effects of exfoliation induced by the laser irradiation and by the presence of air pressure (Figure 3C). The exfoliation increases the surface roughness at about 2–3 microns level, demonstrating that a significant amount of surface defects is produced by the presence of air during the UV laser irradiation.

The laser irradiation of GO produces the removal of the first surface layers of GO leaving the irradiated surface wrinkled with evident exfoliation effects and producing a thinning of the pristine GO foil. The ablation yield, expressed in terms of removed mass per laser pulse, was evaluated as a function of the laser fluence (pulse energy/spot surface) and of the irradiation mode, in air and in vacuum. Its measure can be

done in three different modes: measuring the weight loss of small GO samples after ablation of a certain number of laser pulses; measuring the volume of the ablation crater evaluated with a surface profilometer; using GO foils of known thickness and evaluating the number of laser pulses that cause their perforation. In the first case, employing a laser fluence of 5 mJ/mm², from the mass lost using 100 laser shots, the ablation yield was evaluated of the order of 18 µg/pulse and 21 µg/pulse for irradiation in air and in vacuum, respectively. In the second case, at the same fluence, the conical volume of the ablated crater per laser shot, measured using the surface profiler at a laser fluence of 5 mJ/mm², was determined by a circular spot diameter of 3 mm and area of about 7.07 mm², and a crater depth of about 5 and 6 µm in air and in vacuum, respectively. The ablated mass corresponds to about 18 and 20 µg/pulse, respectively. At the same dose, in the third case, using GO foils of 10 µm (single foil), 20 µm (two overlapping sheets), and 30 µm (three overlapping sheets), the number of laser shots required to pierce the sample was, respectively, of 2, 4, and 6 for the laser irradiation in air and of 2, 4, and 5 for the laser irradiation in vacuum, in agree with a depth ablation of about 5 and 6 microns for irradiation in air and in vacuum, respectively. The three methods have given measurements of ablation yield in perfect agreement between them. Figure 4 reports the experimental data obtained at different laser fluence ablating GO in air and in vacuum environment. The reported measurements are affected by errors of ~5%.

Results indicate that the GO ablation yield due to UV laser ablation grows linearly with the laser fluence. By using the laser pulse energy of about 35.4 mJ and a spot of 7.07 mm², corresponding to a

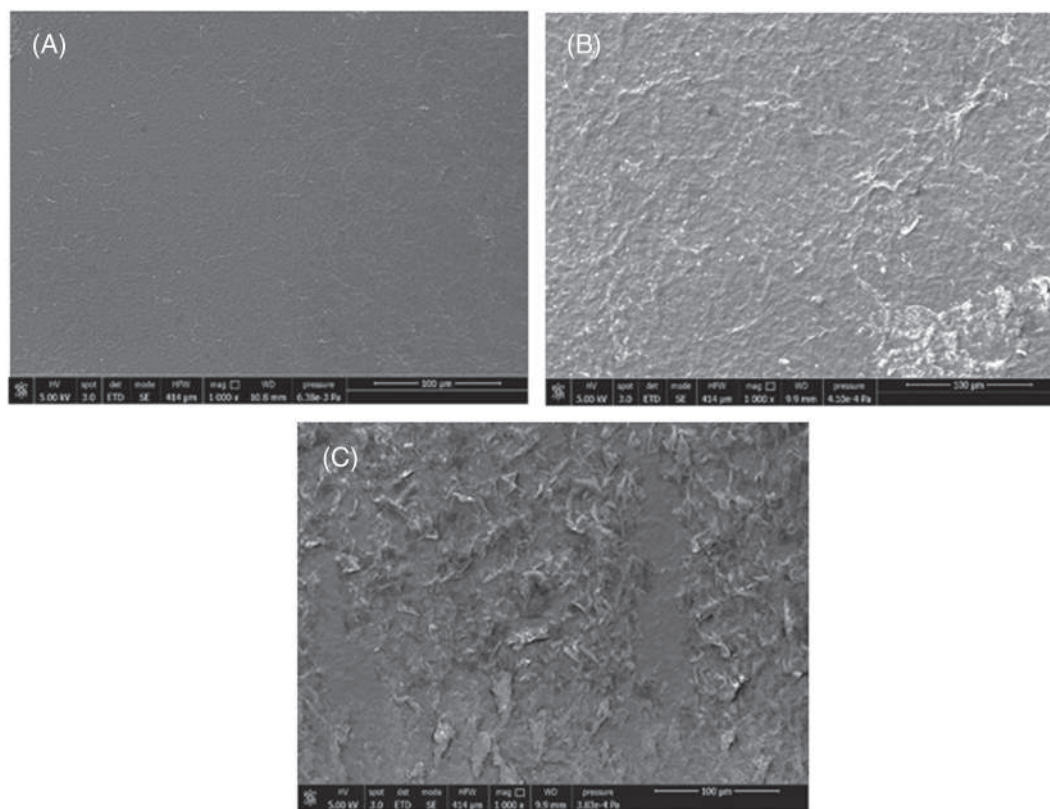


FIGURE 3 Scanning electron microscope (SEM) image of the pristine GO (A) and of the laser irradiated in vacuum (B) and in air (C)

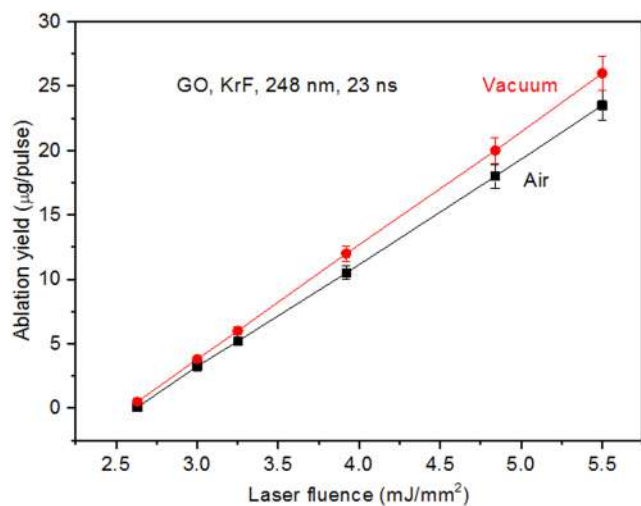


FIGURE 4 Ablation yield of graphene oxide (GO) versus the laser fluence in air and in vacuum conditions

laser fluence of about 5 mJ/mm², the ablation yield in air is 17.5 µg/pulse while in high vacuum, it increases up to about 20 µg/pulse. Thus, the UV laser irradiation in vacuum enhances the effect of GO ablation with respect to air. This can be explained, probably, because of the desorption of the oxygen functional groups and water degassing in vacuum assisted by the laser irradiation producing chemical etching with scission of carbon nanosheets. The ablation yield at the fluence of 5 mJ/mm² in vacuum of 20 µg/pulse at 248 nm wavelength and 23 ns pulse duration corresponds to a removing depth in GO of about 6 µm. This value results significantly higher with respect to that obtained using IR laser operating at 1064 nm, 3 ns pulse duration and 3 mJ/mm² fluence, assuming a value of about 2 µm per laser shot.³³ Of course, the involved process and the pulse duration time are very different in the two cases. The UV ablation is not thermal, but it is a photochemical etching break chemical bonding and promoting their desorption in vacuum. The high penetration depth of UV laser irradiation can be explained by the excessive laser pulse duration of 23 ns with respect to the 3 ns of the IR laser radiation, instead, is a photothermal process producing material removing due to the high thermal process and involving a mass up to a depth due to the thermal diffusion length of the heat in the material. The IR laser irradiation of GO in air, using diode laser operating at 970-nm wavelength and 100-ms pulse duration, shows higher ablation yields evaluated of the order of 3.5–35 µg/pulse depending on the chosen laser pulse energy.³⁴

At the actual stage, it was not possible to separate the ablation yield contribution of water and carbon from the GO sample in air and in vacuum. It should be used a mass spectrometer for the in-vacuum irradiation, for instance, in order to separate the two contributions. However, the irradiation in vacuum favors the desorption of gas phases and molecules split by GO structures due to UV photochemical irradiation and the formation of reduced GO phases. On the contrary, the irradiation in air may promote oxidation phases and increment of the oxygen bonded to the GO structure though the

radical formation during the UV carbon ablation, according to the literature.³⁵ Moreover, in air the water humidity and the nitrogen presence may influence the ablation process and the residual molecules retained in the radiated GO.

The presented data are related to UV irradiation producing photochemical effects in the irradiated GO placed in air or in vacuum. Chemical bonds are broken, and dissociative molecular states are generated. The laser absorption can be based on single and two photon absorption mechanisms, thus, photon energies of about 5 eV (248 nm) and 10 eV (double frequency) released to the GO sample may produce chemical rupture of the bonds C–C (3.6 eV), C–H (4.2 eV), C–O (3.7 eV), C=C (6.4 eV), C≡C (8.7 eV), O–H (4.4 eV), and others.³⁶ In the case of visible and infrared (IR) laser irradiation, instead, photothermal processes are induced with GO thermal desorption of water, oxygen, and other gases and thermal ablation of carbon and other molecular species.^{33–35,37}

The Raman spectroscopy of the pristine and irradiated GO at different laser pulse energies both in air and in vacuum was performed in the shift region of about 400–3500 cm⁻¹.

Figure 5 reports the Raman spectra comparison of irradiation in air, normalizing to the G peak and with the subtracted background, using laser pulses from 5 mJ up to 12.5 mJ, that is, for fluences within 0.7 and 1.75 mJ/mm².

The typical vibrational modes are evident in all the µRaman spectra acquired on different UV laser pulse energy irradiating GO samples between 900 and 2000 cm⁻¹ (D and G peaks) and between 2400 and 3400 cm⁻¹ (2D, D + G and C peaks). The spectra reveal that the laser irradiation determines substantial differences in their characteristics. The two typical vibrational modes of carbon in GO, the G and D peaks, are localized between 900 and 2000 cm⁻¹. The D-mode is caused by the disordered structure of graphene, while the G peak is due to the high frequency E_{2g} phonon at the Brillouin Zone center.³⁸ The second order vibrations of graphene show the 2D and D + G vibrations in the (2600–3000) cm⁻¹ spectral range. The band at about 3100 cm⁻¹ is due to C–H vibrations.³⁹

The fitted spectra allow to determine the parameters that evolve with the laser fluence or laser pulse energy. Among them, the peaks area ratio D/G, (D + G)/G, 2D)/G and (C–H)/G. Such spectra, deconvolved and after background subtraction, allow to evaluate the above-mentioned ratios as a function of the laser fluence or pulse energy for irradiation in air conditions (23°C, 1 atm and 40% air humidity).

Such ratios were reported in the plot of Figure 6 as a function of the laser pulse energy for the four spectra reported in Figure 5, indicating an evident growth in the case of the D/G peak yield ratio, that is, an increment of the disorder of the GO structure with the laser fluence. This increment is high at 5-mJ pulse energy, reaching about the 45% with respect to the pristine value, while it is of about 35% for higher laser pulse energies. The (D + G)/G ratio does not change significantly with the laser pulse energy. The increment with the energy is observed also for the 2D/G ratio but it is less evident than for D/G one due to the overlapping with the other near vibration bands. Its increment is about 35% at 5 mJ and stabilizes at about 16% at higher

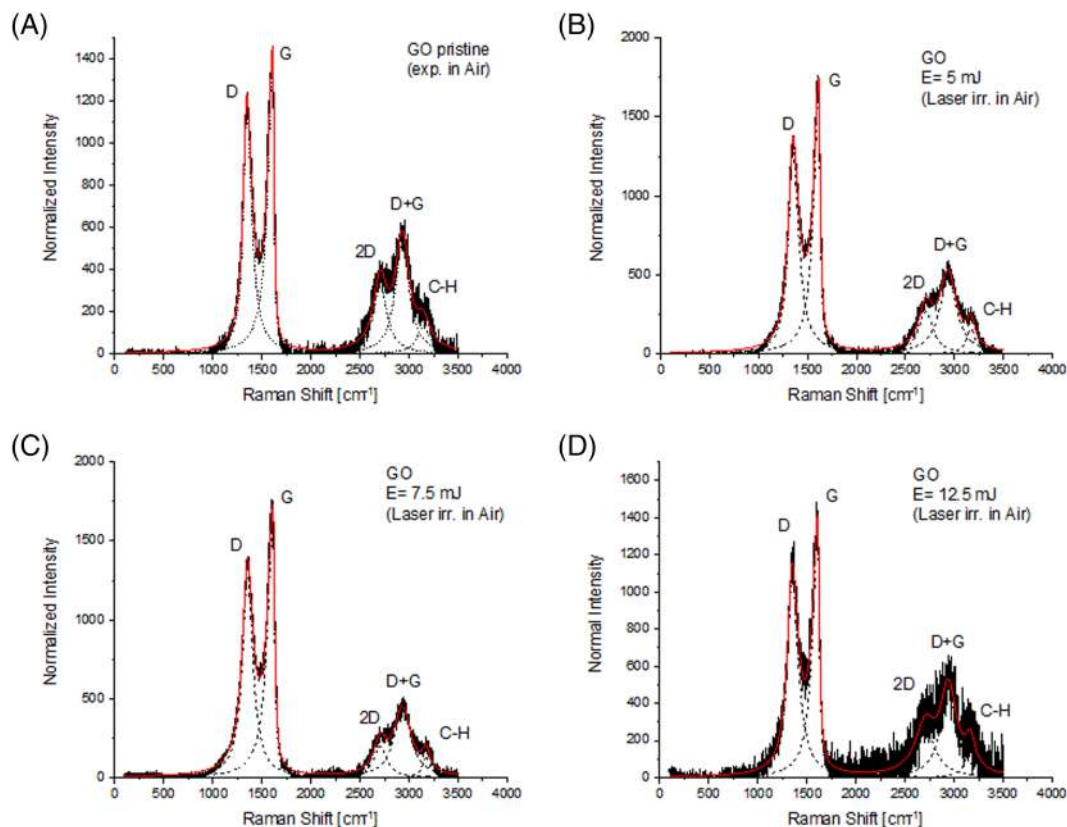


FIGURE 5 Normalized Raman spectra comparison for graphene oxide (GO) irradiated in air

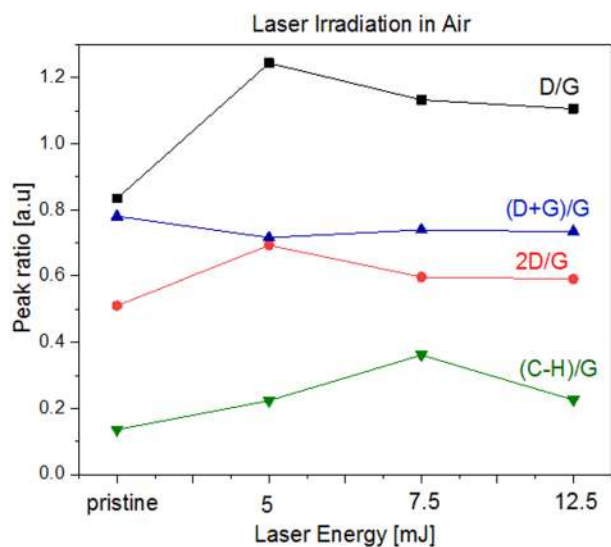


FIGURE 6 Peak yield ratios (b) vs. laser pulse energy for graphene oxide (GO) irradiated in air

laser pulse energy. The (C–H)/G ratio increases with the laser pulse energy, probably as result of the formation of new chemical bonds between the target carbon atoms and the hydrogen present in the air in the form of humidity.

In agreement with the literature, the irradiation in vacuum of GO shows different results with respect to the case of the irradiation in air.²⁶ Figure 7 shows the Raman spectra comparison of UV laser irradiation in vacuum, normalizing to the G peak and subtracting the fitted background, using laser pulses from 2.5 mJ up to 7.5 mJ, that is, for fluences within 0.35 and 1.05 mJ/mm². Also, in this case spectra permit to evaluate the peak yield ratios D/G, (D + G)/G, 2D/G, and (C–H)/G as a function of the laser irradiation conditions. By the fitted spectra, it was possible determine the parameters that evolve with the laser fluence or laser pulse energy at a vacuum condition of 10^{–5} mbar and 23°C temperature. Also in this case the D peak yield increases with the laser fluence, as demonstrated by the D/G ratio increment with the laser pulse energy, indicating that a damage of the graphene structure is produced by the UV laser in vacuum. However, the damage is lower with respect to the in-air irradiation, in fact the maximum D/G ratio increases of about 18% at 2.5 mJ with respect to the pristine value and stabilizes at an increment of about 10% at higher pulse energies. In this case the (D + G)/G ratio increases significantly with the laser pulse energy indicating an increment of the disorder of the GO produced by the UV laser irradiation in vacuum. A small increment with the energy is observed also by the 2D/G ratio, but it is less evident than for D/G one. Its maximum increment is about 37.5% at the maximum used laser energy of 7.5-mJ energy. The (C–H)/G ratio, instead, decreases with the laser pulse energy, as expected. In fact, the UV laser irradiation in vacuum liberates water

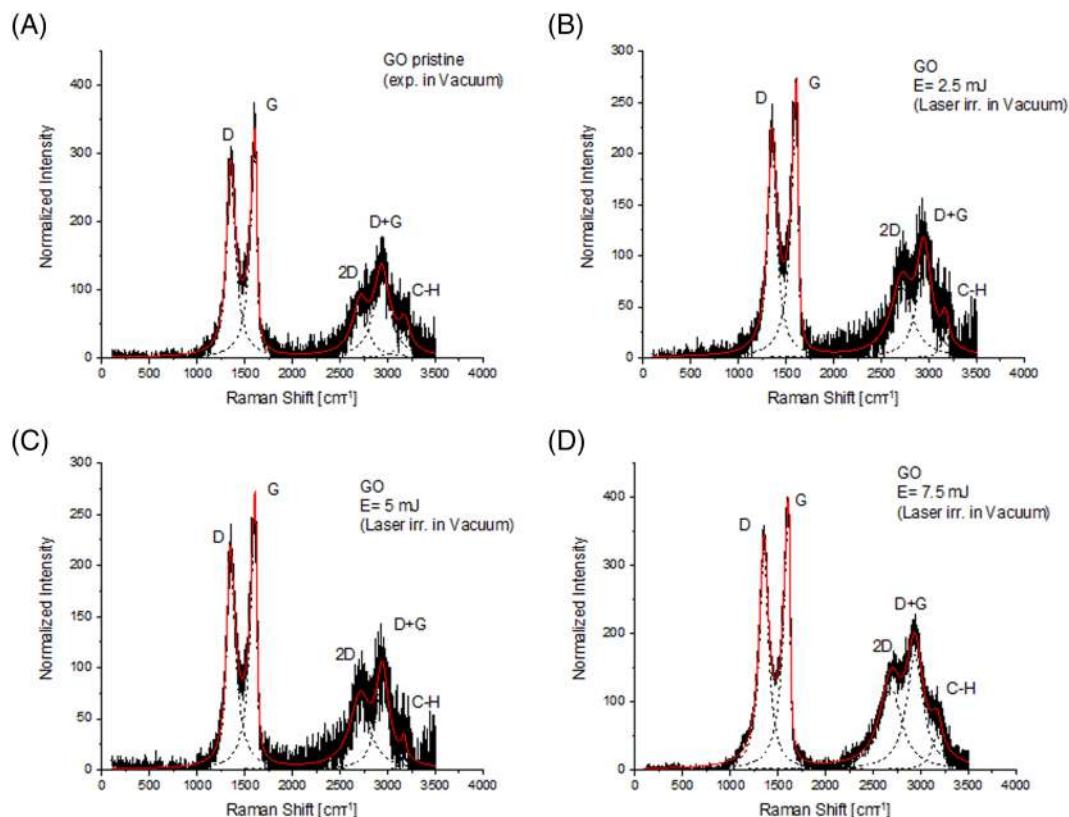


FIGURE 7 Normalized Raman spectra comparison for graphene oxide (GO) irradiated in vacuum

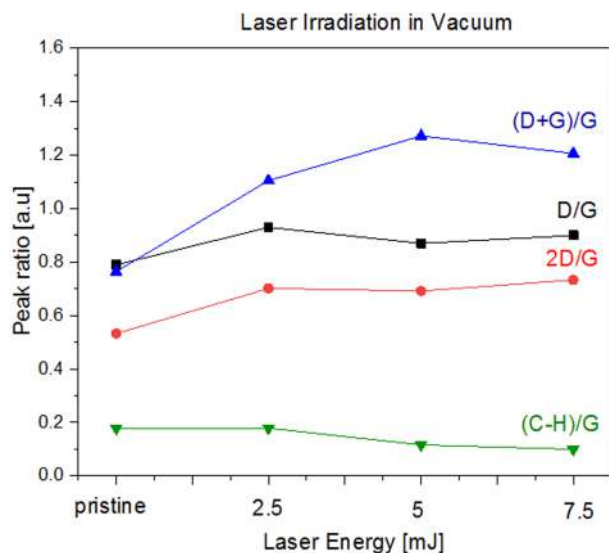


FIGURE 8 Peak yield ratios (b) vs. laser pulse energy for graphene oxide (GO) irradiated in vacuum

and functional groups of oxygen, especially the hydroxylic group (C—OH) and the carboxylic group (O=C—OH), reducing the C—H content of the graphene sample, according to the literature.⁴⁰ Such ratios were shown in the plot of Figure 8, for a comparison of the yield versus the laser energy in vacuum.

Thus, the comparison between Figures 6 and 8 shows that the in-air irradiation produces a significant increment of the D/G, 2D/G and (C—H)/G ratios, indicating that high structural modifications of the graphene order with increment of the C—H molecules bonded to the structures occurs with the UV laser irradiation. The in-vacuum irradiation reduces the damage to the graphene structures and decreases the C—H chemical bonds, as indicated by the D/G and (C—H)/G Raman yield ratios.

4 | DISCUSSION AND CONCLUSIONS

The paper reports some data about the excimer laser ablation in air and in vacuum of GO foils with thickness of the order of 10 microns. The results indicate that the ablation in vacuum is more effective with respect that in air, probably due to the desorption and sublimation of water and other functional groups of oxygen removed by the photoablative process occurring in vacuum. The ablation process also in absence of thermal processes develops effects of exfoliation at the residual GO surface, as evinced by electron microscopy. The effect of layer removal of GO for the used fluence is of the order of 10 $\mu\text{g}/\text{pulse}$. Considering the large laser spot of 3 mm in diameter and using the density of 3.6 g/cm^3 , this ablation corresponds to the removing of a thickness of about 0.39 μm . Thus, using a laser fluence of 5 mJ/mm^2 , from Figure 4, it is possible to evince a removing of a thickness of about 0.7 μm in air and of about 0.8 μm in vacuum. The high layer

removing with respect to the laser penetration depth of the order of 63 nm indicates that the ablation process occurs continuously during the laser pulse duration of 23 ns. The produced plasma, dense but under-critical, permits the laser transparency and the continuum removing of GO monolayers, especially in vacuum conditions.

Further investigations concerning the structure of GO modified by the laser irradiation in air and in vacuum were conducted using micro Raman spectroscopy of the irradiated surfaces. It demonstrates that the D peak grows with the laser pulse energy and that the disorder of the graphene in the GO sheets enhances both in air and in vacuum with an excess of disorder in the case of vacuum with respect to air irradiations. Another observation is devoted to the laser wavelength of 248 nm corresponding to photons of about 5 eV in energy. In regime of photo-dissociation, the photon energy is able to break the chemical bond C—C (3.6 eV) and the C—O (3.7 eV).⁴¹ Single photon absorption does not permit to break the C=C bond (6.26 eV) and the stronger C≡C, C=O (8.6 eV) and C≡O bonds³²; however, at high laser intensity, the multiphoton absorption effect with two photon absorption may reach the energy sufficient to break these strong chemical bonds generating reactive free radicals. These aspects explain the high ablation yield and the effect of exfoliation shown by the GO irradiated surfaces. Presented results can be used for applications of treated GO surface by UV laser beams in order to define controlled modifications in the structure due to photo-ablative and not photo-thermal processes, such those occurring using IR and visible lasers. The modified layers can be controlled by the laser energy and fluence and by the very low penetration depth of the used UV radiation.

ACKNOWLEDGMENTS

The authors thank the INFN, Gr. V, Project CIMA, for the useful support given to the realization of this research by the INFN sections of Lecce and Catania. Open Access Funding provided by Università del Salento within the CRUI-CARE Agreement.

ORCID

Alfio Torrissi  <https://orcid.org/0000-0003-2404-5062>

Lorenzo Torrissi  <https://orcid.org/0000-0003-0853-136X>

REFERENCES

- Wang K, Ruan J, Song H, et al. Biocompatibility of graphene oxide. *Nanoscale Res Lett*. 2011;6(1):1-8.
- Poulin P, Jalili R, Neri W, et al. Superflexibility of graphene oxide. *PNAS*. 2016;113(40):11088-11093.
- Silipigni L, Salvato G, Di Marco G, et al. Band-like transport in high vacuum thermal reduced graphene oxide films. *Vacuum*. 2019;165:254-261.
- Joshi RK, Alwarappan S, Sahajwalla V, Yoshimura M, Nisina Y. Graphene oxide: the new membrane material. *Appl Mater*. 2015;1(1):1-12.
- Dimiev AM, Eigler S. *Graphene Oxide: Fundamentals and Applications*. New York: John Wiley & Sons; 2016:147-174.
- Torrissi L, Silipigni L, Salvato G. Graphene oxide/Cu junction as relative humidity sensor. *J Mater Sci Mater Electron*. 2020;31(14):11001-11009.
- Torrissi L, Silipigni L, Manno D, et al. Investigations on graphene oxide for ion beam dosimetry applications. *Vacuum*. 2020;178:109451-109458.
- Yang JW, Yu ZY, Cheng SJ, et al. Graphene oxide-based nanomaterials: an insight into retinal prosthesis. *Int J Mol Sc*. 2020;21(8):2957-2973.
- Xu S, Zhang L, Wang B, Ruoff RS. Chemical vapor deposition of graphene on thin-metal films. *Cell Rep*. 2021;2(3):100372-100407.
- Rahman MR, Rashid MM, Islam MM, Akanda MM. Electrical and chemical properties of graphene over composite materials: a technical review. *Mater Sci Res*. 2019;16(2):142-163.
- Torrissi L, Cutroneo M, Havranek V, et al. Self-supporting graphene oxide films preparation and characterization methods. *Vacuum*. 2019;160:1-11.
- Zhu Y, Murali S, Cai W, et al. Graphene and graphene oxide: synthesis, properties, and applications. *Adv Mater*. 2010;22(35):3906-3924.
- Huang XM, Liu LZ, Zhou S, Zhao JJ. Physical properties and device applications of graphene oxide. *Front Phys*. 2020;15(3):3301-1-3301-70.
- Kumar SK, Modak MD, Paik P. Graphene oxide for biomedical applications. *J Nanomed Res*. 2017;5(6):1-6, 00136.
- Galante C, Gao W, Mathkar A, et al. Science and engineering of graphene oxide. *Particle*. 2014;31(6):619-638.
- Torrissi L, Silipigni L, Calcagno L, Cutroneo M, Torrissi A. Carbon-based innovative materials for nuclear physics applications (CIMA), INFN Project. *Radiat Eff Defects Solids*. 2021;176(1-2):100-118.
- Cutroneo M, Havranek V, Mackova A, et al. Selective modification of electrical insulator material by ion micro beam for the fabrication of circuit elements. *Radiat Eff Defects Solids*. 2020;175(3-4):307-317.
- Boretti A, Al-Zubaidy S, Vaclavikova M, Al-Abri M, Castelletto S, Mikhalovsky S. Outlook for graphene-based desalination membranes. *NPJ Clean Water*. 2018;5(1):1-11.
- Giorgi R, Baglioni M, Berti D, Baglioni P. New methodologies for the conservation of cultural heritage: micellar solutions, microemulsions, and hydroxide nanoparticles. *Acc Chem Res*. 2010;43(6):695-704.
- Manno D, Serra A, Buccolieri A, et al. Structural and spectroscopic investigations on graphene oxide foils irradiated by ion beams for dosimetry application. *Vacuum*. 2021;188:1-10, 110185.
- Zhang Y, Chung TS. Graphene oxide membranes for nanofiltration. *Curr Opin Dent*. 2017;16:9-15.
- Smith AT, LaChance AM, Zeng S, Liu B, Sun L. Synthesis, properties, and applications of graphene oxide/reduced graphene oxide and their nanocomposites. *NMS*. 2019;1(1):31-47.
- Cutroneo M, Torrissi L, Havranek V, et al. Localized modification of graphene oxide properties by laser irradiation in vacuum. *Vacuum*. 2019;165:134-138.
- Longo A, Verucchi R, Aversa L, et al. Graphene oxide prepared by graphene nanoplatelets and reduced by laser treatment. *Nanotechnology*. 2017;28(22):1-8, 224002.
- Orabona E, Ambrosio A, Longo A, Carotenuto G, Nicolais L, Maddalena P. Holographic patterning of graphene-oxide films by light-driven reduction. *Opt Lett*. 2014;39(14):4263-4266.
- Torrissi L, Cutroneo M, Silipigni L, Fazio M, Torrissi A. Effects of the laser irradiation on graphene oxide foils in vacuum and air. *Phys Solid State*. 2019;61(7):1327-1331.
- Choudhury FA, Ryan ET, Nguyen HM, Nishi Y, Shohet JL. Effects of ultraviolet (UV) irradiation in air and under vacuum on low-k dielectrics. *AIP Adv*. 2016;6(7):1-4, 075012.
- Yang CR, Tseng SF, Chen YT. Laser-induced reduction of graphene oxide powders by high pulsed ultraviolet laser irradiations. *Appl Surf Sci*. 2018;444:578-583.
- Graphenea, High quality graphene producer, actual website 2021 (last access: 16/09/2021): <https://www.graphenea.com/>

30. Smausz T, Kondasz B, Gera T, Ajtai T. Determination of UV-visible-NIR absorption coefficient of graphite bulk using direct and indirect methods. *Appl Phys A Mater Sci Process*. 2017;123(10):1-7.
31. Overall NJ. Confocal Raman microscopy: common errors and artefacts. *Analyst*. 2010;135(10):2512-2522.
32. Fityk software, actual website 2021 (last access: 16/09/2021): <https://fityk.nieto.pl>
33. Torrisi L, Silipigni L, Cutroneo M. Laser effects on graphene oxide irradiated in high vacuum. *Radiat Eff Defects Solids*. 2018;173(1-2): 73-84.
34. Torrisi L, Cutroneo M, Torrisi A, Salvato G, Proverbio E, Silipigni L. Reduction of graphene oxide foils by IR laser irradiation in air. *JINST*. 2020;15(03):1-14, C03006.
35. Torrisi L, Silipigni L, Cutroneo M. Radiation effects of IR laser on graphene oxide irradiated in vacuum and in air. *Vacuum*. 2018;153: 122-131.
36. Bobrinetskiy II, Emelianov AV, Otero N, Romero PM. Patterned graphene ablation and two-photon functionalization by picosecond laser pulses in ambient conditions. *Appl Phys Lett*. 2015;107(4): 043104
37. Sadoqi M, Kumar S, Yamada Y. Photochemical and photothermal model for pulsed-laser ablation. *J Thermophys Heat Trans*. 2002;16(2): 193-199.
38. Tuinstra F, Koenig JL. Raman spectrum of graphite. *J Chem Phys*. 1970;53(3):1126-1130.
39. Ferrari AC, Basko DM. Raman spectroscopy as a versatile tool for studying the properties of graphene. *Nat Nanotechnol*. 2013;8(4): 235-246.
40. Silipigni L, Fazio M, Fazio B, Cutroneo M, Torrisi L. Tailoring the oxygen content of graphene oxide by IR laser irradiation. *Applied Physics a*. 2018;124(545):1-12.
41. Rumble JR. *Handbook of Chemistry and Physics*. 102nded. Florida: CRC; 2021.

How to cite this article: Torrisi A, Velardi L, Serra A, Manno D, Torrisi L, Calcagnile L. Graphene oxide modifications induced by excimer laser irradiations. *Surf Interface Anal*. 2022;54(5): 567-575. doi:10.1002/sia.7066